ACADEMIA ROMÂNĂ
Revue Roumaine de Chimie
http://web.icf.ro/rrch/

Rev. Roum. Chim.,
2018, *63*(10), 931-939

QSAR TECHNIQUES ON SEVERAL BORTEZOMIB COMPOUNDS AS PROTEASOME INHIBITOR ANTICANCER DRUG

Robabeh SAYYADIKORD ABADI[*,a] and Asghar ALIZADEHDAKHEL[b]

[a] Department of Chemistry, Rasht Branch, Islamic Azad University, Rasht, IRAN
[b] Department of Chemical Engineering, Rasht Branch, Islamic Azad University, Rasht, Iran

Received December 7, 2017

The activity of the 25 derivatives of Bortezomib was performed by multiple linear regression (MLR),artificial neural network (ANN) as modeling tools and simulated annealing (SA) and genetic algorithm (GA) techniques as optimization methods. The obtained results from combinations of modelling-optimization methods were compared and GA-ANN combination showed the best performance according to its correlation coefficient and mean sum square errors (RMSE). In MLR-MLR, SA-ANN, MLR-GA and GA-ANN methods observed root mean sum square errors(RMSE) of 0.2831, 0.0457, 0.0623 and 0.0349 in the gas phase and 0.3925, 0.0749, 0.0928 and 0.0317 in the solvent phase respectively (N=25). The results obtained using the GA-ANN method indicated that the activity of derivatives of Bortezomib depends on different parameters including L1p, R6v, SP03, BEle6, GATS6m, G1m and JGI6 descriptors in the gas phase and X1A, TI2, Mor18m, Mor15m, SP06, RDF155e and Mor17p descriptors in the solvent phase.

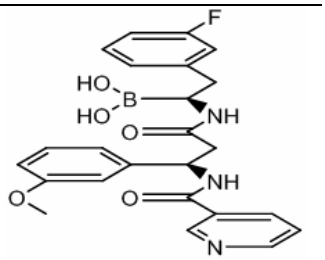

INTRODUCTION

The first proteasome inhibitor was Bortezomib which was approved by the US FDA for the treatment of newly diagnosed multiple myeloma and relapsed/refractory multiple myeloma as well as mantle cell lymphoma.[1–2] The complex multiple mechanisms involved in the anticancer activity of Bortezomib through proteasome inhibition has not been fully elucidated. Degradation of anti-apoptotic proteins and prevention of degradation of pro-apoptotic proteins, which results in programmed cell death in malignant cells, are carried out through proteasome inhibition.

Bortezomib is important in the treatment of multiple myeloma. It is also being investigated for the treatment of other hematological malignancies and solid tumors as a single agent or as part of a combined therapy.[3-5,6–7]

One of the most efficacious approaches for designing new chemical identities and understanding the action mechanisms of drugs is quantitative structure activity relationship (QSAR).[8-11]

To find a set of molecular descriptors including constitutional, geometrical, topological, quantum chemical with a higher impact on the biological activity of interest is the first step in a typical QSAR study.[12-15] There are several variable selection models including multiple linear regression (MLR), genetic algorithm (GA), simulated annealing algorithm (SA) *etc*.[15-19] One of the most efficacious computational approaches for the inspection of inhibition mechanism is quantitative structure activity relationship studies (QSAR).[16,17]

In the current study, we have applied multiple linear regressions (MLR), simulated annealing (SA), genetic algorithm (GA) and artificial neural networks (ANN) as linear and nonlinear approaches to investigate QSAR in Bortezomib compounds as anticancer drugs. The QSAR methods have also been used to select more effective descriptors that are required to obtain a hybrid computational model for a

* Corresponding author: sayyadi@iaurasht.ac.ir

rough prediction of inhibitory activity. The ability of these methods to predict the inhibitor activity of Bortezomib compounds as anticancer drugs has also been compared.

COMPUTATIONAL METHODS

Geometry optimizations of Bortezomib compounds were carried out with B3lyp/6-31 using Gaussian 03W.[20] Polarized continuum model (PCM) was applied to examine non-specific solvent effect, and all molecules were optimized in H_2O solvent.

Dragon program was used for calculation of 3226 molecular descriptors including topological, geometrical, MoRSE,[22,23] RDF,[23,24] GETAWAY,[15,25] auto-correlations[12] and WHIM[26,27] groups for each of the[25] compounds[21] and then SPSS program was used to reduce the number of descriptors through an objective feature selection in three steps.

These steps include: **(**i) descriptors having the same value, at least 70% of compounds were removed; (ii) descriptors with correlation coefficient less than 0.25 with the logarithm half maximal inhibitory concentration (-log IC_{50}) as the dependent variables were considered and removed;[12] (iii) by carrying out these two-steps, the number of descriptors were reduced to 776 and 805 in the gas and solvent phase respectively and then a stepwise multiple linear regression procedure was employed to select the best of the 776 and 805 descriptors. Low standard deviation, least numbers of independent variables, high ability for prediction and high F statistical value,[28] high correlation coefficient (R) and RMSE are characteristics of an ideal model, where the RMSE is defined as follows:

$$RMSE = \sqrt{\frac{\sum_{i=1}^{n}(y_i - y_o)^2}{n}} \qquad (1)$$

where y_i is the desired output, y_o is the predicted value by the model, and n is the number of molecules in the data set.

In QSAR methods including GA-ANN, SA--ANN, MLR-SA, MLR-GA, 776 and 805 descriptors in gas and solvent phase were considered as possible input of the ANN and fed into the input layer of the ANNs. In this study, they were all three-layer and Levenberg-Marquart algorithm[29] was applied for training on the TSET members. (Fig. 1). Modelling and optimization calculations were carried out using Matlab. 7.12. These networks were supposed to identify the non-linear relationship between the structural descriptors and inhibitory activity of Bortezomib compounds.

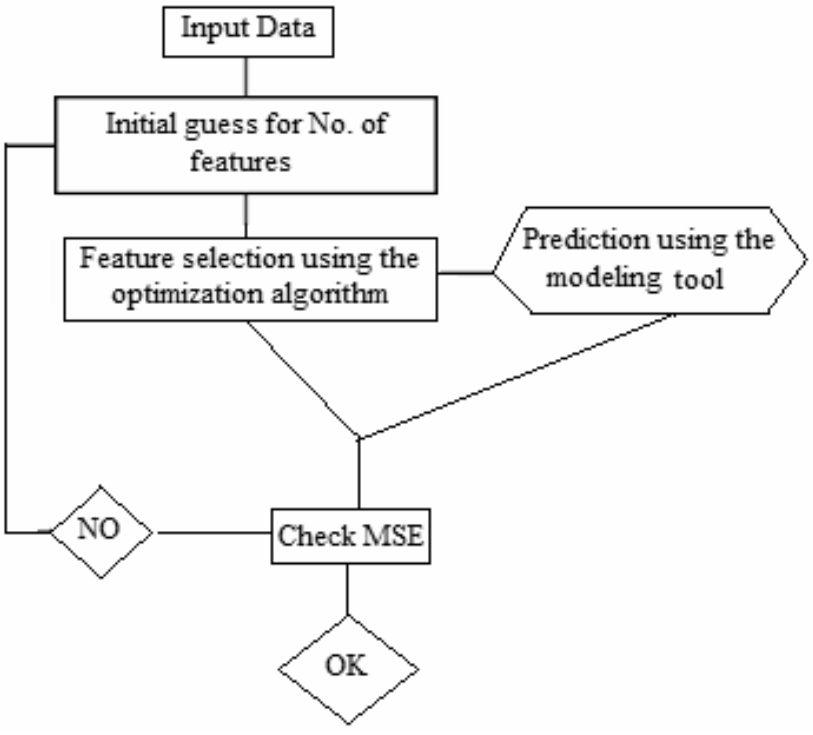

Fig. 1 – The employed procedure for finding optimum descriptors.

RESULTS AND DISCUSSION

Twenty-five different Bortozomib derivatives were selected as sample set and geometry of the complexes were optimized using Gaussian 03W at B3LYP/6-31g. Polarized continuum model (SCRF) was applied to examine non-specific solvent effect, and all molecules were optimized in H_2O solvent. All studied Bortezomib compounds are presented in Figure 2.

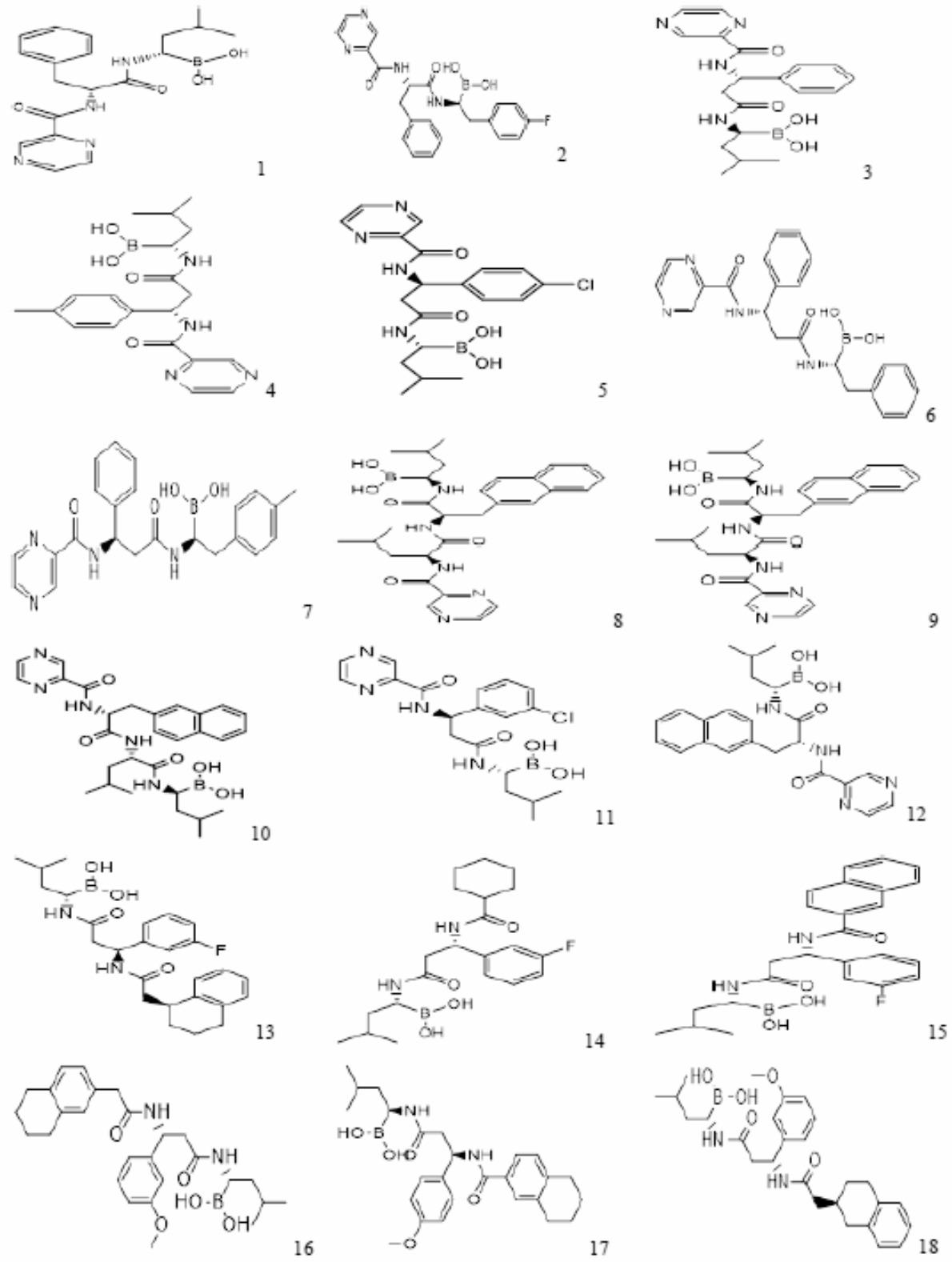

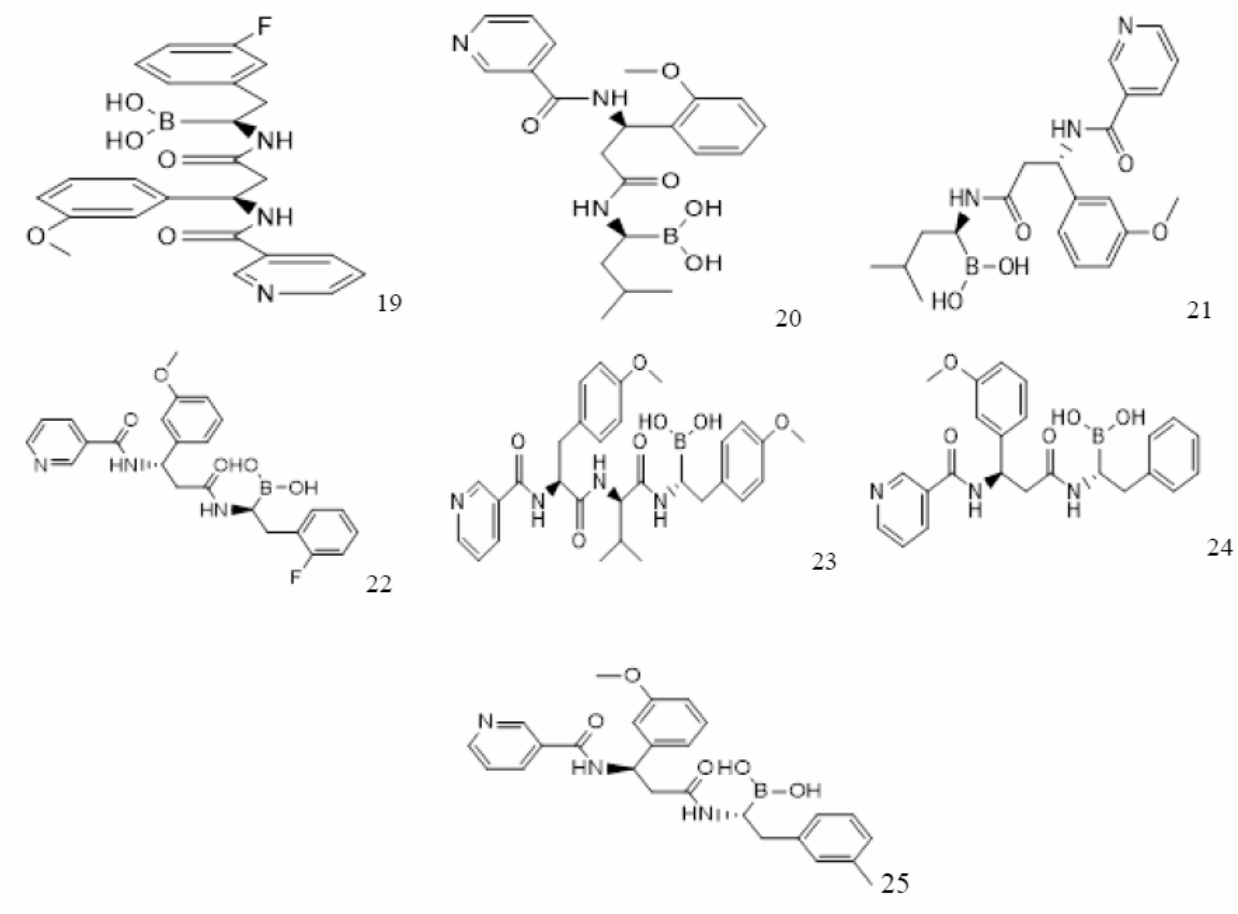

Fig. 2 – Optimized structure of the compounds used to build QSAR models with B3lyp/6-31g in gas phase.

Table 1

Statistical parameters of different linear QSAR models in the gas and solvent phases

QSAR Model	R^2	RMSE
MLR-PLS1 gas	0.9308	0.2836
MLR-PCR gas	0.8977	0.3448
MLR-MLR gas	0.93105	0.2831
MLR-PLS1 solvent	0.7417	0.5480
MLR-PCR solvent	0.7289	0.5613
MLR-MLR solvent	0.8674	0.3925

Table 2

Statistical parameters of different non-linear QSAR models in the gas and solvent phases

QSAR Models	Predicted		Train	
	R^2	RMSE	R^2	RMSE
SA-ANN (GAS)	0.9623	0.0457	0.9659	0.0377
SA-ANN (SOLVENT)	0.9398	0.0749	0.9564	0.0547
MLR-GA (GAS)	0.9473	0.0623	0.9691	0.0371
MLR-GA (SOLVENT)	0.9245	0.0928	0.9664	0.0475
GA-ANN(GAS)	0.9728	0.0349	0.9706	0.0442
A-ANN (SOLVENT)	0.9743	0.0317	0.9636	0.0409

Table 3

The best selected descriptors using MLR-MLR Method for the gas phase

Descriptor	Definition	Type
MATS5m	Moran autocorrelation – Lag 5/Weighted by atomic massses	2D autocorrelations
BELm2	Lowest eigenvalue n.2 of Burden matrix / Weighted by atomic massses	Burden eigenvalues
HOMA	Harmonic Oscillator model of aromaticity index	Geometrical descriptors
RDF 105m	Radial Distribution function -10.5/ Weighted by atomic massses	RDF descriptors
Mor 30p	3D-MORSE-Signal 30/Weighted by atomic polarizabilities	3D-MoRSE descriptors
H-051	H-attached to alpha -C	Atom –centred fragments
BO8[N-O]	Presence/ absence of N-O at topological distance 08	2D binary fingerprints

Linear and nonlinear feature selection models were used to select the most significant descriptor (stepwise-MLR, SA and GA). According to the types of variable selection model and feature mapping techniques, these models were shown as MLR-MLR, MLR-ANN, SA-ANN, MLR-GA and GA-ANN.

The SPSS[30] software which was used for the model processing in MLR method is presented in Table 2. When the MLR-MLR method was used, the RMSE for predicted activity was found to be 0.2831 in the gas phase and 0.3925 in the solvent phase. In addition, the correlation coefficient (R^2) calculated for the PSET was 0.9310 in the gas phase and 0.8644 in the solvent phase. It shows that the MLR-MLR method is better than the other linear methods (MLR-PLS1 and MLR-PCR, Table 1).The definition of the descriptors in the MLR-MLR model is shown in Table 3.

The 776 and 805 descriptors in gas and solvent phase were fed to the SA-ANN, GA-ANN and MLR-GA models and then the best descriptors were selected (Table 5-10).

MATS5m (Tables 3, 4) and MATS5v, GATS6e (Table 5) and ATS6p, GATS8e (Table 6) and GATS7p (Table 7) and MATS7e (Table 8) and GATS6m (Table 9) are 2D autocorrelation descriptors. The 2D-autocorrelation descriptors show the topological structure of the Bortezomib compounds, which in nature are more complex than the classical topological descriptors.[31]

Gu1 (Table 6), L1p (Table 9), G1m (Table 9) are WHIM descriptors. WHIM descriptors in compounds were built in such a way that they can capture the relevant molecular 3D information regarding compound size, shape, symmetry and atom distribution with respect to invariant reference frames.[32]

BElm2 (Tables 3, 4) and BELe6 (Table 9) are burden eigenvalues descriptors. The other group of descriptors was the highest eigenvalue of burden matrix, which was determined as eigenvalues of burden matrix (B). The number of atoms and bond order between two atoms or the electronegativity of the atoms are shown by the B matrix.[32]

HOMA (Table 3) and G(N…O) (Table 7) are geometrical descriptors that incorporate information on the magnitude of the displacement between the polarized field (center of charge) and the molecular centroid (center of mass).[23]

Table 4

The best selected descriptors using MLR-MLR method for the solvent phase

Descriptor	Definition	Type
MATS5m	Moran autocorrelation – Lag 5/Weighted by atomic massses	2D autocorrelations
BELm2	Lowest eigenvalve n.2 of Burden matrix / Weighted by atomic massses	Burden eigenvalues
RDF 105m	Radial Distribution function -10.5/ Weighted by atomic massses	RDF descriptors
Mor 30p	3D-MORSE-Signal 30/Weighted by atomic polarizabilities	3D-MoRSE descriptors
H-051	H-attached to alpha -C	Atom –centred fragments
BO8[N-O]	Presence/ absence of N-O at topological distance 08	2D binary fingerprints
F07[N-O]	Frequency of N-O at topological distance 07	2D-frequency fingerprints

Table 5

The best selected descriptors using SA-ANN method for the gas phase

Descriptor	Definition	Type
MATS5v	Moran autocorrelation-lag5/weighted by atomic Van der waals volumes	2Dautocorrelations
GATS6e	Geary autocorrelation-lag6/weighted by atomic San derson electronegativities	2Dautocorrelations
X2Av	Average valence connectivity index chi-2	Connectivity indices
SP20	Shape profile no.2	Randic molecular profiles
RDF155u	Radial Distribution Function-15.5/unweighted	RDF descriptors
TI2	Second Mohar index TI2	Topological descriptors
npyrazines	Number of Pyrazines	Functional group count

Table 6

The best selected descriptors using SA-ANN method for the solvent phase

Descriptor	Definition	Type
D/Dr10	Distance/detour ring index of order 10	Topological descriptors
ATS6P	Broto-Moreau autocorrelation of a topological structure-lag6/Weighted by atomic polarizabilities	2D autocorrelations
GATS8e	Geary autocorrelation-lag8/Weighted by atomic Sanderson electronegativities	2D autocorrelations
Gu	G total symmetry index/unweighted	WHIM descriptors
Mor13m	3D-MoRSE-signal 13/Weighted by atomic masses	3D-MoRSE descriptors
F10[C-B]	Frequency of C-B at topological distance 10	2D frequency fingerprints
H8u	H autocorrelation of lag 8/ unweighted	GETAWAY descriptors

Table 7

The best selected descriptors using MLR-GA method for the gas phase

Descriptor	Definition	Type
GATS7p	Moran autocorrelation-lag7/weighted by atomic polarizabilities	2D autocorrelation
VDA	Average vertex distance degree	Topological descriptors
B08[N-O]	Presence/absence of N-O at topological distance 0.8	2D binary fingerprints
EEig01r	Eigenvalue 01 from edge adj.matrix weighted by resonance integrals	Edge adjacency indices
G(N…O)	Sum of geometrical distances between N-O	Geometrical descriptors
nAB	Number of aromatic bonds	Constitutional descriptors
B05[N-B]	Presence/absence of N-B at topological distance 0.5	2D binary fingerprints

Table 8

The best selected descriptors using MLR-GA method for the solvent phase

Descriptor	Definition	Type
Mor30e	3D-MoRSE-Signal 30/Weighted by atomic Sanderson electronegativities	3D-MoRSE descriptors
Mor09m	3D-MoRSE-Signal 09/Weighted by atomic masses	3D-MoRSE descriptors
ECC	eccentricity	Topological descriptors
MATS7e	Moran autocorrelation-lag7/weighted by atomic Sanderson electronegativities	2D autocorrelation
F05[N-B]	Frequency of N & at topological distance 05	2D frequency fingerprints
B10[N-N]	Presence/absence of N-N at topological distance 10	2D binary fingerprints
H7u	H autocorrelation of lag 7/unweighted	GETAWAY descriptors

Table 9

The best selected descriptors using GA-ANN method for the gas phase

Descriptor	Definition	Type
L1p	1st component size directional WHIM index/Weighted by atomic polarizabilities	WHIM descriptors
R6v	R autocorrelation of lag 6/Weighted by atomic van der Waals volumes	GETAWAY descriptors
SP03	Shape profile no.03	Randic molecular profiles

Table 9 (continued)

BEle6	Lowest eigenvalue n.6 of Burden matrix/Weighted by atomic Sanderson electrone gativities	Burden eigenvalues
JGI6	Mean topological charge index of order 6	Topological charge indices
GATS6m	Geary autocorrelation-lag6/Weighted by atomic masses	2D autocorrelations
G1m	1 st component symmetry directional WHIM index /Weighted by atomic masses	WHIM descriptors

Table 10

The best selected descriptors using GA-ANN method for the solvent phase

Descriptor	Definition	Type
X1A	Average connectivity index ch-i	Connectivity indices
TI2	Second Mohar index TI2	Topological descriptors
Mor 18m	3D-MoRSE-Signal 18/Weighted by atomic masses	3D-MoRSE descriptors
Mor15m	3D-MoRSE-Signal 15/Weighted by atomic masses	3D-MoRSE descriptors
SP06	Shape profile no.6	Randic molecular profiles
RDF155e	Radial Distribution Function-15.5/Weighted by atomic Sanderson electronegativities	RDF descriptors
Mor17P	3D-MoRSE-Signal 17/Weighted by atomic polarizabilities	3D-MoRSE descriptors

RDF 105 m (Tables 3, 4) and RDF 155u (Table 5) and RDF155e (Table 10) are RDF descriptors. The radial distribution function (RDF) descriptors, which are based on the distance of distribution in the molecule and ensemble of n atoms, can be interpreted as the probability distribution of finding an atom in a spherical volume of radius R.[32]

Mor30p (Tables 3, 4) and Mor13m (Table 6) and Mor 30e (Table 8) and Mor18m, Mor15m (Table 10) are 3D-MoRSE descriptors. The molecular transformation employed in electron diffraction studies created the 3D-MoRSE descriptors.[29]

TI2 (Tables 5, 10) and VDA (Table 7) and ECC (Table 8) and D/Dr10 (Table 6) are topological descriptors. Topological index encode information mathematically regarding the structure of molecules, and are sensitive to size, shape, branching, cyclicity.[32]

F07 [N-O] (Table 4) and F10[C-B] are 2D frequency fingerprints descriptors. These descriptors, which are referred to as fingerprints, are used for substructure searching and as input for analysis on molecular similarity.[32]

X2Av (Table 5), X1A (Table 10) are connectivity indices descriptors which are used for molecular structure quantitation in which weighted counts of substructure fragments and structural features, such as size, branching, unsaturation, heteroatom content and cyclicity are encoded.[23]

EEig01r (Table 7) is the edge adjacency indices for molecular graphs that have been used to define a new topographic index. The novel index is computed considering the molecules as weighted graphs. The elements of the edges are substituted by the bond orders between connected atoms in the molecule wherever they set.[31]

The number of aromatic bonds (nAB) represents the number of bonds with a bond order of 1.5.[33]

H8u (Table 6) and H7u (Table 6) and R6v (Table 9) are GETAWAY (Geometry, Topology, and Atom Weights Assembly) descriptors. These descriptors in compounds encode the geometrical information obtained from the molecular matrix, the topological information obtained from the molecular graph and the information obtained from atomic weights which are specially designed with the aim of matching the 3D-molecular geometry.[32]

SP20 (Table 5) and SP03 (Table 9) and SP06 (Table 10) are Randic molecular profiles .B08 [N-O] (Tables 3, 4, 7) and B10 [N-N] (Table 8) are 2D binary fingerprints.[32]

The statistical parameters of all QSAR approaches are presented in Tables 1 and 2. In trained neural networks a computation of 80% Bortozomib compounds is used in the GA-ANN model, the RMSE and R-square were calculated as 0.0349 and 0.9728 in the gas phase, and 0.0317 and 0.9743 in the solvent phase for predicted activity respectively.

Therefore, the results obtained demonstrated that the GA-ANN model produced better results with good predictive ability than other models in Bortezomib compounds and as such, only the descriptors used in this model were evaluated in this study. These descriptors are shown in Tables 9 and 10. The plot showing the variation between observed and predicted –logIC50 values are shown in Figures 3 and 4.

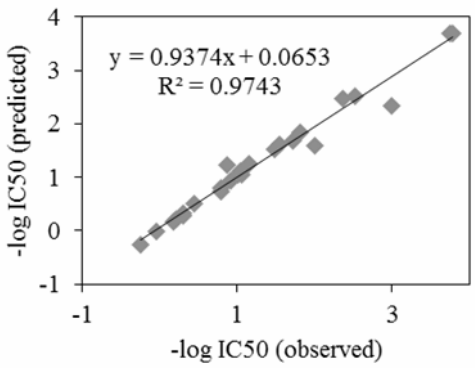

Fig. 3 – Predicted *vs.* observed values of –log(1/IC50) for the gas phase.

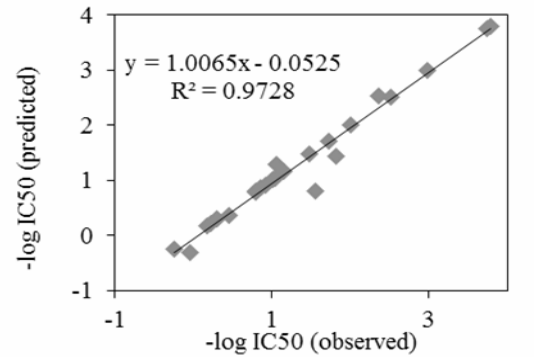

Fig. 4 – Predicted *vs.* observed values of –log(1/IC50) for the solvent phase.

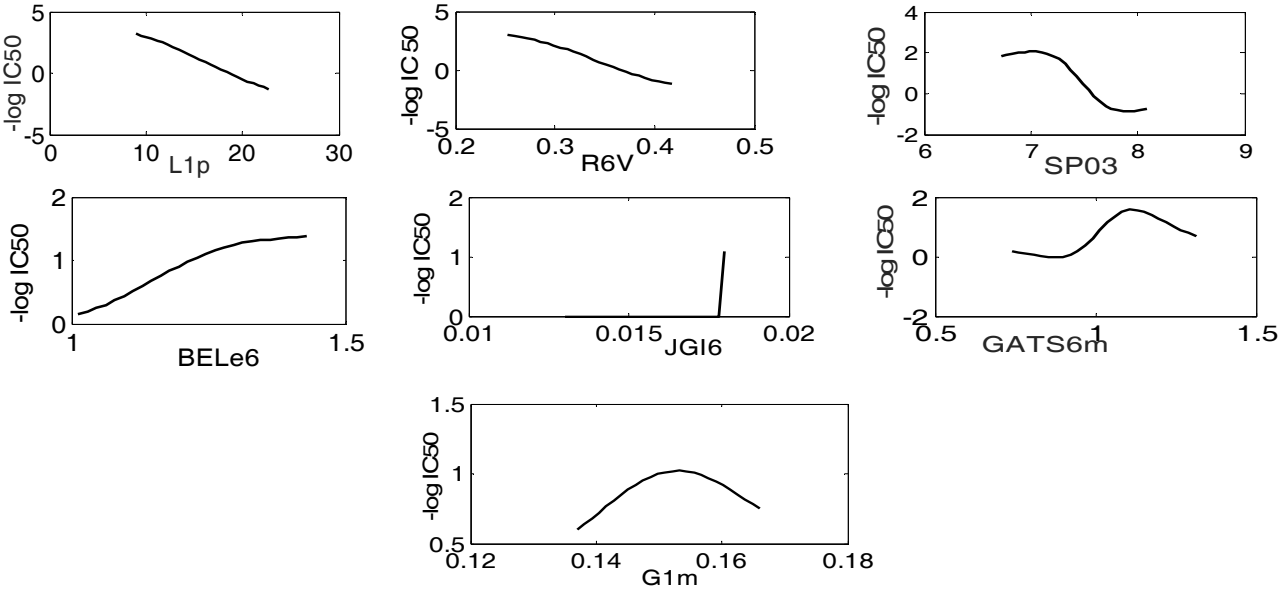

Fig. 5 – –log IC50 values *versus* selected descriptors in the gas phase.

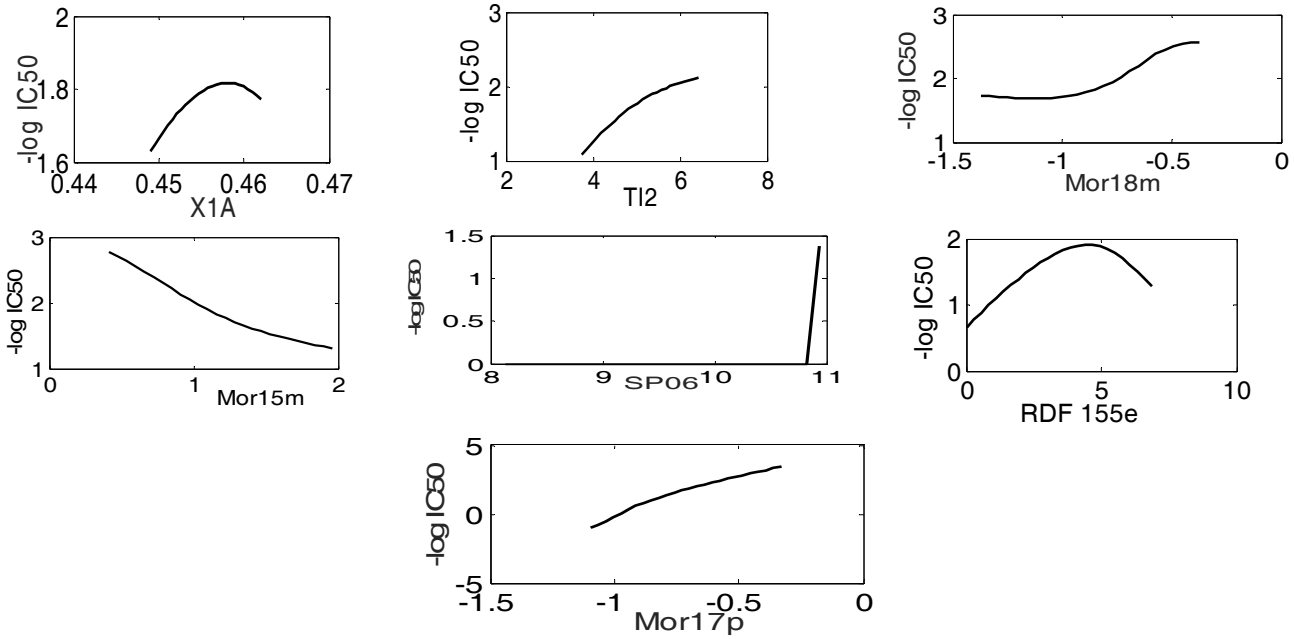

Fig. 6 – –log IC50 values *versus* selected descriptors in solvent phase.

Plots of the L1p, R6v, SP03, BELe6, JGI6, GATS6m and G1m (Factor 1, 2, 3, 4, 5, 6 and 7) descriptors in the gas phase (Fig. 5) and the X1A, TI2, Mor18m, Mor15m, SP06, RDF 155e and Mor17p (Factors 1,2,3,4,5,6 and 7) descriptors in the solvent phase (Fig. 6) *versus* –logIC50 experimental results were plotted using Matlab program.

Charts in the gas phase showed that an increase in the amount of the L1p, R6v, SP03 descriptors brought about a decrease in the amount of –logIC50 experimental. Increase in GATS6m and G1m descriptors at first resulted in an increase and then a decrease in the –logIC50 experimental. An increase in the amount of BELe6 descriptor resulted in an increase in –logIC50 experimental. Increase in the amount of the JGI6 descriptor between 0.017 and 0.018 produced no change in the amount of –logIC50 experimental. During this period, a bar will be seen in the –logIC50 experimental.

Charts in solvent phase showed that an increase in X1A, TI2, Mor18m, RDF 155e, Mor15m, SP06, and Mor17p (Factors 1, 2, 6 and 7) descriptors resulted in an increase in response. Increase in Mor18m descriptor (Factor 3) up to a value of 1 did not produce much change in response, and then from quantity 1 to the peak, the response increased. An increase in Mor15m descriptor (Factor 4) brought about a decrease in the response content. There was no change in response following an increase in the SP06 descriptor (Factor 5) between 10.5 and 11. During this period, a rising bar will be seen in the response. Thus, descriptors that increase response and reduce the amount of IC_{50} are more effective.

CONCLUSIONS

Although a large number of nonlinear and hybrid approaches could be employed to establish QSAR models, GA-ANN model was admittedly one of the best QSAR models. The results obtained also showed that L1p , R6v , SP03 , BELe6 , GATS6m , G1m,JGI6 descriptors in the gas phase and X1A, RI2, Mor15m, Mor18m, SP06, RDF155e and Mor17p descriptors in the solvent phase were more significant than other descriptors in building this QSAR model and also in predicting the biological activity of Bortezomib substitution patterns.

Acknowledgement. The support provided by Islamic Azad University of Rasht is gratefully acknowledged.

REFERENCES

1. R. C. Kane, P. F. Bross, A. T. Farrell and R. Pazdur**,** *Oncologist*, **2003**, *8*, 508.
2. R. C. Kane, R. Dagher, A. Farrell, CW. Ko, R. Sridhara, R. Justice and R. Pazdur, *Clin. Cancer Res*., **2007**, *13*, 5291.
3. JR. Berenson, H. H.Yang, K. Sadler, SG. Jarutirasarn, RA.Vescio, R. Mapes, M. Purner, SP. Lee, J. Wilson, B. Morrison, J. Adams, D. Schenkein and R. Swift, *J. Clin. Oncol*., **2006,** *24*, 937 .
4. RC . Kane , AT.Farrell ,R. Sridhara and R. Pazdur., *Clin. Cancer Res*., **2006**, *12*, 2955.
5. QP. Dou and RH. Goldfarb, *IDrugs,* **2002**, 5, 828.
6. RI. Fisher, SH.Bernstein, BS. Kahl, B. Djulbegovic, MJ.Robertson, S. de Vos, E. Epner, A. Krishnan, JP. Leonard, S. Lonial, EA. Stadtmauer, OA. O'Connor, H. Shi, AL. Boral and A. Goy*, J. Clin. Oncol*., **2006**, *24*, 4867.
7. CN .Papandreou, DD.Daliani, D. Nix, H. Yang, T. Madden, X. Wang, CS.Pien, RE. Millikan, L. Pagliaro , J. Kim, J. Adams, P. Elliott, D. Esseltine, A. Petrusich, P. Dieringer, C. Perez and CJ. Logothetis, *J. Clin. Oncol***. 2004**, *22*, 2108.
8. S.Y. Liao, J.C. Chen, L. Qian, Y. Shen and K.C. Zheng., *Mol. Inform.*, **2008,** *27*, 280 .
9. X. Wang, W. Yang, X. Xu, H. Zhang and Y. S. Wang., *Curr. Med. Chem*., **2010**, *17*, 2788.
10. J. Wan, L. Zhang and GF. Yang, *J. Comput. Chem.,* **2004**, *25*, 1827.
11. HK. Srivastava, FA. Pasha and PP. Singh, *Int., J. Quantum. Chem*. **2005**, *103*, 237.
12. D. Horvath and B. Mao., M*ol. Inform.***, 2003**, *22,* 498.
13. S. Putta, J. Eksterowicz, C. Lemmen and R. Stanton*., J. Chem. Inf. Comput. Sci***., 2003**, *43*, 1623.
14. S.Gupta, M. Singh and A. K. Madan, *J. Chem. Inf. Comput. Sci*., **1999**, *39*, 272.
15. V. Consonni, R. Todeschini and M. Pavan., *J. Chem. Inf. Comput. Sci*., **2002**, *42*, 693 -705.
16. D.A. Winkler*., Briefings in Bioinformatics*, **2002**, *3*, 73.
17. R. Guha, J. R. Serra and P.C. Jurs., *J. Mol. Graph. Model.*, **2004,** *23*, 1.
18. S. Kirkpatrick, Jr.C.D. Gelatt and M. P. Vecchi., *Science*, **1983**, *220*, 671.
19. V.O. Cerný., *Journal of Optimization Theory and Applications*, **1985**, *45*, 41.
20. E. B. DeMelo and M.M. Ferreira. , *Eur. J. Med.Chem*. **, 2009,** *44*, 3577.
21. R. Todeschini and V. Consonni, *Commun. Math. Comput. Chem.*, **2010**, 64, 359–372.
22. J.H. Schuur.,P. Selzer and J. Gasteiger.*,J. Chem. Inf. Comput. Sci.*, **1996**, *36*, 334.
23. R. Todeschini and V. Consonni, "Handbook of Molecular Descriptors", Wiley-VCH*.,* 2000**.**
24. M.C. Hemmer. V. Steinhauer and J. Gasteiger*., Vibr Spectrosc*, **1999**, *19*,151.
25. V.Consonni, R.Todeschini and M. Pavan., *J .Chem. Inf. Comput .Sci***., 2002**, *42*, 682.
26. P. Gramatica, V. Consonni and R. Todeschini, *Chemosphere,* **1999**, *38* , 1371.
27. P.Gramatica, V. Consonni and R. Todeschini, *Chemosphere*, **2000,** *41*, 763.
28. M.H. Fatemi and S. Gharaghani., *Bioorg. Med. Chem.*, **2007**, *15*, 7746.
29. M. Jalali-Heravi and F. Parastar., *J. Chem. Inf. Comput. Sci.,* **2000**, *40*, 1470.
30. K. Levenberg, *Quart. Appl. Math.*, **1944**, *2*, 164.
31. SPSS, Version 19, available at http://www.spssscience.com. **2010**.
32. T. Asadollahi, S. Dadfarnia, A. M. Haji Shabani, J.B. Ghasemi, *MATCH Commun. Math. Comput. Chem***., 2014**, *71*, 287.